Published in final edited form as:
J Cell Biochem. 2009 October 15; 108(3): 577–588. doi:10.1002/jcb.22289.

Interleukin-6 Maintains Bone Marrow-Derived Mesenchymal Stem Cell Stemness by an ERK1/2-Dependent Mechanism

Katie L. Pricola[*,1], **Nastaran Z. Kuhn**[*], **Hana Haleem-Smith**, **Yingjie Song**, and **Rocky S. Tuan**[2]

Cartilage Biology and Orthopaedics Branch, National Institute of Arthritis and Musculoskeletal and Skin Diseases, National Institutes of Health, Department of Health and Human Services, Bethesda, Maryland 20892, USA

Abstract

Adult human mesenchymal stem cells (MSCs) hold promise for an increasing list of therapeutic uses due to their ease of isolation, expansion, and multilineage differentiation potential. To maximize the clinical potential of MSCs, the underlying mechanisms by which MSC functionality is controlled must be understood. We have taken a deconstructive approach to understand the individual components *in vitro*, namely the role of candidate "stemness" genes. Our recent microarray gene expression profiling data suggest that interleukin-6 (IL-6) may contribute to the maintenance of MSCs in their undifferentiated state. In this study, we showed that *IL-6* gene expression is significantly higher in undifferentiated MSCs as compared to their chondrogenic, osteogenic, and adipogenic derivatives. Moreover, we found that MSCs secrete copious amounts of IL-6 protein, which decreases dramatically during osteogenic differentiation. We further evaluated the role of IL-6 for maintenance of MSC "stemness", using a series of functional assays. The data showed that IL-6 is both necessary and sufficient for enhanced MSC proliferation, protects MSCs from apoptosis, inhibits adipogenic and chondrogenic differentiation of MSCs, and increases the rate of *in vitro* wound healing of MSCs. We further identified ERK1/2 activation as the key pathway through which IL-6 regulates both MSC proliferation and inhibition of differentiation. Taken together, these findings show for the first time that IL-6 maintains the proliferative and undifferentiated state of bone marrow-derived MSCs, an important parameter for the optimization of both *in vitro* and *in vivo* manipulation of MSCs.

Keywords

Mesenchymal stem cells; Differentiation; Stemness; Interleukin-6

Three components are required for successful tissue engineering and regeneration: cells with regenerative potential, a biocompatible scaffold or matrix, and environmental and endogenous influences to drive these cells towards desired functional tissue neo-genesis. Adult human mesenchymal stem cells (MSCs) are a promising source of cells that can largely satisfy the first of our three necessary criteria. MSCs are tissue-resident stem cells [Pereira et al., 1995; Prockop, 1997]. They are commonly isolated from the bone marrow but can also be found in the perivascular regions of most tissues, such as adipose, skeletal muscle, and umbilical cord

2Correspondence: Rocky S. Tuan, Ph.D., Cartilage Biology and Orthopaedics Branch, National Institute of Arthritis and Musculoskeletal and Skin Diseases, National Institutes of Health, 50 South Drive, Room 1140, MSC 8022, Bethesda, Maryland 20892-8022, USA, Telephone: 301-451-6854, Fax: 301-435-8017, tuanr@mail.nih.gov.
*Authors contributed equally to this work
1Current Address: Stanford University School of Medicine, Palo Alto, California, USA

[Sarugaser et al., 2005; Zuk et al., 2002]. MSCs are capable of differentiation into several cell lineages, including osteoblasts, chondrocytes, adipocytes, and myoblasts [Jiang et al., 2002; Pittenger et al., 1999]. Owing to their ease of isolation, expansion, and multi-lineage differentiation capability, MSCs are a promising cell source for both tissue engineering and *in vivo* stimulation of other tissue-resident stem cells. In addition, MSCs possess immunosuppressive activities and have been successfully used to treat Graft vs. Host Disease [Le Blanc et al., 2004] and as a source for gene therapy (Osteogenesis Imperfecta) [Le Blanc et al., 2005].

Although there is vast potential for MSCs, both future and realized, current limitations include the small number of cells that can be harvested from a primary source and the inconsistent proliferation and differentiation capabilities across patients. A better understanding of the intrinsic gene regulation and the external environmental stimuli and cues governing MSC fate decisions will enhance both our understanding of MSC biology and our ability to promote MSC self-renewal and readiness to differentiate. We have recently taken a deconstructive approach into understanding the influence of individual cues *in vitro*, namely identification of candidate "stemness" genes. Our microarray data [Song et al., 2006] suggest that interleukin-6 (IL-6), a cytokine highly expressed in the bone marrow stroma [Ogasawara et al., 1996] and known for its role in bone homeostasis [Manolagas, 1995], may be responsible for maintenance of MSCs in the undifferentiated state. Specifically, we reported *IL-6* down-regulation in MSCs during differentiation and up-regulation during de-differentiation or the return to a more stem-like state [Song et al., 2006]. The additional role of IL-6 as a secreted signaling factor makes this an interesting gene to study both for its intrinsic and extrinsic effects. In this study, we have assessed the role of IL-6 in maintenance of MSC "stemness" by investigating its effects on proliferation, apoptosis, differentiation, and *in vitro* wound healing activity in human bone marrow-derived MSCs.

MATERIALS AND METHODS

Materials

Cell culture media and reagents were purchasedfrom Invitrogen (Carlsbad, CA). All other chemicals were purchased from Sigma-Aldrich (St. Louis, MO) unless specified otherwise.

Isolation and *In Vitro* Expansion of MSCs

MSCs were isolated from femoral heads harvested during electivetotal hip arthroplasty in consenting patients (N=8, ages 39–72) (IRB approval - University of Washington). All samples were from individuals with osteoarthritis that do not have rheumatoid arthritis, or other autoimmune or inflammatory diseases, or congenital deformities. For our studies, bone marrow-derived MSCs were expanded *in vitro* in basalmedium (BM), consisting of high glucose Dulbecco's Modified Eagle's Medium, 10% lot-selected (Invitrogen, catalog # 12662029, lot # 1160485) MSC-qualified fetal bovine serum (FBS), and antibiotic/antimycotic. BM was replaced 72 h after initial plating to select for plastic-adherent cells and weekly thereafter. Confluent cultures (~1.2×10^4 cells/cm^2) were passaged at 1:3; all experiments were performed at passage 4. Previous phenotypical analysis of MSCs at passage 4 has been reported to show that they are acceptable as culture-expanded MSCs with multilineage potential [Song and Tuan, 2004].

Differentiation of MSCs

MSCs were induced to undergo osteogenic, adipogenic, and chondrogenic differentiation as previously described [Song and Tuan, 2004].

Osteogenesis—To stimulate osteogenic differentiation, cells were plated at 1.5×10^4 cells/cm^2 and BM was supplemented with 10 nM dexamethasone, 10 mM β-glycerophosphate,50 μg/ml ascorbate phosphate, and 10 nM 1,25 dihydroxyvitamin D_3.

Adipogenesis—To induce adipogenesis, cells were plated at 4.0×10^4 cells/cm^2 and BM was supplemented with 1 μM dexamethasone, 1 μg/mlinsulin, and 0.5 mM 3-isobutyl-1-methylxanthine.

Chondrogenesis—In order to induce chondrogenesis, cells were cultured asa high-density pellet culture (2.5×10^5 cells/pellet) in serum-free BM supplemented with0.1 μM dexamethasone, 50 μg/ml ascorbate phosphate,40 μg/ml L-proline, 100 μg/ml sodium pyruvate, 1%ITS-premix, and 10 ng/ml transforming growth factor-β3(TGF-β3) (R&D Systems, Minneapolis, MN). RNA was harvested at days 3, 7, 14, and 21 for all three differentiated lineages.

Human IL-6 ELISA Assay

IL-6 protein levels in culture supernatants were measured using commercial ELISA kits (eBioscience, San Diego, CA). The ELISA assay was conducted per the manufacturer's instructions at room temperature unless indicated otherwise. Briefly, ELISA plates were coated with the capture antibody and incubated overnight at 4°C. Wells were washed extensively and then blocked for 1 h. The wells were incubated for 2 h with human Il-6 standards and supernatants from MSCs either in BM and osteogenic induction medium, which were diluted 1:100 in order to obtain measurements within the standard curve. After extensive wash steps, wells were incubated with detection antibody for 1 h and then washed several more times. Wells were incubated with Avidin-HRP for 30 min, washed extensively, incubated with substrate solution for 15 min, followed by the addition of stop solution, and A_{450} values were measured using a microplate reader.

Growth and Proliferation Assay

MSCs were plated at 1.5×10^4 cells/cm^2 in serum-free BM with or without 10 ng/mL human recombinant IL-6 (R&D Systems, Minneapolis, MN), 10 μM of the MEK1/2 inhibitor, U0126, solubilized in 0.1% dimethylsulfoxide (DMSO) carrier, both U0126 and IL-6, or DMSO carrier alone. Growth and proliferation were assessed in parallel by hemacytometer counting and by thiazolyl blue tetrazolium bromide (MTT) proliferation assay at 1, 2, and 3 days post-plating. For counting, each condition was plated in triplicate and duplicate counts of trypan blue negative cells per well were averaged (mean + SD). In parallel plates, 1.25 mg/mL per well MTT reagent was added, incubated at 37°C for 2 h, solubilized with DMSO, and A_{540} values of the eluant measured using a microplate reader.

siRNA Knockdown

MSCs were transfected with 25 μg of gene-specific siRNA or negative scramble control according to manufacturer specification using a BTX-ECM 830 Electroporator and siPORT Electroporation buffer (Ambion, Austin, TX). Following transfection, cells were plated for proliferation assays and RNA harvest at the same densities described elsewhere.

In Situ Cell Death Assay

Undifferentiated MSCs were seeded at 1.2×10^4 cells/cm^2 and grown for 72 h in serum-free medium with or without IL-6 (10 ng/mL). After 72 h, cells were fixed in 4% buffered paraformaldehyde, permeabilized with 0.1% Triton-X100, incubated with the TUNEL reaction mixture (Roche, Indianapolis, IN) and nuclear-counterstained with DAPI. Apoptosis was evaluated by epifluorescence microscopy (475/35 nm excitation and 530/43 nm emission

filters). Relative levels of apoptosis were quantified by calculating the percentage of TUNEL positive cells at the center of each well. Field images with approximately equivalent numbers of positive cells in both control and sample populations were merged to assess both location and intensity of TUNEL staining as well as the size and appearance of nuclei (Leica DMRB microscope and Hamamatsu C4742-95 digital camera; IPLab software).

Real-time RT-PCR Microarray Analysis

Undifferentiated MSCs were seeded at 1.5×10^4 cells/cm^2 and cultured under serum-free conditions with or without IL-6 (10 ng/mL) for 72 h (n=3 each). RNA was harvested using Trizol reagent (Invitrogen) and purified with RNeasy Mini kit (Qiagen, Valencia, CA), and cDNA was synthesized using RT2 First Strand Kit according to the RT^2 Profiler PCR Array System (Super Array Bioscience, Frederick, MD). For each sample, cDNA synthesized from 0.5 μg starting RNA and RT2 SYBR Green master mix were loaded into 96-well pathway-specific PCR array plates containing probes for 84 genes in the apoptotic pathways and 12 controls. Plates were run in an iCycler iQ real-time PCR detection system (Bio-Rad, Hercules, CA) using the manufacturer's protocol, and results were analyzed using the RT^2 Profiler PCR Array Data Analysis web portal. Using cut-off criteria, a 2.75-fold induction or repression of expression was considered to be significant.

Analysis of MSC Differentiation

Osteogenesis was detected at day 10 by alkalinephosphatase (ALP) histochemistryand ALP activity assay. Briefly, ALP Yellow (pNPP) Liquid Substrate for ELISA was used, and enzyme activity was normalized to DNA content with Quanti-iT™ Pico Green dsDNA Assay Kit (Invitrogen). At day 18, calcium deposition/matrix mineralization was assessed by Alizarin Red stain, and staining was quantified spectrophotometrically (A_{405}) after solubilization with 5% SDS in 0.5N HCl. Adipogenesis was detected at day 18 by presence of Oil Red O stained cytoplasmic lipid droplets and assessed quantitatively by counting stained cells and grading stain intensity. To assess chondrogenicdifferentiation at day 21, high-density cell pellets were fixed with 4%paraformaldehyde and 8 μm cryosections were stained for sulfated proteoglycan with Alcian Blue(pH 1.0) as described previously [Song and Tuan, 2004]. Sulfated glycosaminoglycans (sGAG) were quantified using the Blyscan assay kit (BioColor, UK) after digestion with 300 μg/mL papain. Bound 1, 9- dimethyl-methylene blue was released and quantified spectrophotometrically (A_{656}), and total sGAG calculated from a chondroitin 4-sulfate standard curve. Total sGAG was normalized to DNA content as described above. Real-time reverse transcription-polymerase chain reaction(RT-PCR) was used to analyze expression levels of *ALP* and osteocalcin(*OC*) for osteogenesis, lipoprotein lipase (*LPL*) and fatty acid binding protein-4 (*FABP4*) for adipogenesis, and aggrecan (*AGC*) and collagen type II (*COL2A1*) for chondrogenesis (see below for details).

Differentiation of MSCs in the Presence of IL-6

MSCs were differentiated as described above with or without IL-6 (10 ng/mL). Secondarily, to assess the effect of IL-6 pre-treatment, undifferentiated MSCs were grown with or without IL-6 (10 ng/mL), U0126 (10 μM) or both for three days prior to induction of differentiation. RNA was harvested at day 3, 7, 14, 21 and differentiation was analyzed as described above.

Gene Expression Analysis by Real-time RT-PCR

Total RNA was prepared from monolayer and pellet cultures using Trizol reagent (Invitrogen) and purified with RNeasy Mini-kit (Qiagen). cDNA was synthesized using SuperScriptIII first-strand synthesis system (Invitrogen). Ten nanograms of cDNA were amplified and detected using iQ-SYBR Green supermix and 10 μM F+R primer mix in an iCycler iQ real-time PCR detection system. For all real-time RT-PCR experiments, gene expression levels were

normalized to an internal glyceraldehyde-3-phosphate dehydrogenase(*GAPDH*) control and averaged from triplicate samples. Primers used included: ***IL-6,*** 5′-cagttgccttctccctggg-3′, 5′-tgagtggctgtctgtgtggg- 3′ [Seck et al., 2002]; ***OC,*** 5′-gcctttgtgtccaagc-3′, 5′-ggaccccacatccatag-3′; ***LPL,*** 5′-gagatttctctgtatggcacc-3′, 5′-ctgcaaatgagacactttctc-3′; ***FABP4,*** 5′-tgggccaggaatttgacgaagt-3′,5′-tcaacgtcccttggcttatgct-3′; ***ALP,*** 5′-tcagaagctcaacaccaacg-3′, 5′-gtcagggacctgggcatt-3′; ***AGC,*** 5′-tgcgggtcaacagtgcctatc-3′, 5′-cacgatgcctttcaccacgac-3′; ***COL2A1,*** 5′-ggaaactttgctgcccagatg-3′, 5′-tcaccaggttcaccaggattgc-3′; ***GAPDH,*** 5′-caaggctgagaacgggaagc-3′, 5′-aggggggcagagatgatgacc-3′ All primer sequences listed after IL-6 were previously published [Nesti et al., 2008].

In Vitro Wound Healing Assay

MSCs were plated at 2.0×10^4 cells/cm^2 and grown in BM until near 100% confluence. At the time of initial wounding (defined here as 0 h), scratches were made in the cell monolayer with a 200 μl pipette tip. After wounding, each well was rinsed with low serum BM (2% FBS). Control wells were replenished with low serum BM; IL-6 treated wells were replenished with 10 ng/mL IL-6 in low serum BM. A total of 30 defects (control, N=12; IL-6, N=18) in cultures derived from two different patients were followed over the course of 18 h. These time points were specifically chosen to be shorter than the doubling time reported for human bone marrow-derived MSCs [Conget and Minguell, 1999], such that any observed effects are due to cell migration and not cell proliferation. Images were captured using a Zeiss Axio Observer A.1 microscope and Axiovision Rel. 4.6 software, and blinded measurements were made at 0, 6, 12, and 18 h time-points using the interactive measurement line tool scaled to the 5× objective.

Western Blot Analysis

MSCs plated at 1.5×10^4 cells/cm^2 and grown to 80% confluence in BM were switched to serum-free medium for 12–15 hrs prior to treatment and protein harvest. After treatment with IL-6 and/or U0126, cells were rinsed with cold PBS and lysed in RIPA buffer, 0.1% SDS containing 1% IGEPAL Ca-630, and a cocktail of protease inhibitors- Complete, EDTA-free protease inhibitor cocktail (Roche) and Halt-Phosphatase Inhibitor cocktail (Pierce, Rockford, IL). Fifteen μg of sample protein, nonphosphorylated, and phosphorylated STAT3 and STAT1 control cell extracts were run on 10% SDS-Tris-HCl Ready Gels (Bio-Rad), transferred onto PVDF membrane (Bio-Rad) and probed for β-actin (Sigma), STAT3, phospho-STAT3, STAT1, phospho-STAT1, ERK1/2, phospho-ERK1/2 (all antibodies from Cell Signaling, Danvers, MA). Expression was detected with the Amersham ECL system (Piscataway, NJ) and SuperSignal (Pierce).

Statistical Analysis

All data are presented as mean ± SD unless otherwise specified. Statistical significance was calculated by Student's t-test was used for pairwise comparisons and one-way ANOVA was used for multiple comparisons (Software used was SPSS 16.0; Specific parameters used were the General Linear Model, Univariate Analysis: One-way ANOVA with Tukey Post Hoc Analysis). Statistical significance was analyzed on data from at least three independent experiments on three different patient samples performed in triplicate. p values < 0.05 were defined as significant (* $p < 0.05$, ** $p < 0.01$, *** $p < 0.001$).

RESULTS

IL-6 Expression is Down Regulated during MSC Differentiation

Previously, our laboratory reported that MSC expression of *IL-6* decreases during lineage-specific differentiation [Song et al., 2006]. To validate our previous microarray data, we compared the levels of *IL-6* mRNA by real-time RT-PCR in undifferentiated MSCs and their

differentiated counterparts- osteoblasts, adipocytes, and chondrocytes (Figure 1A). *IL-6* message levels were significantly greater in undifferentiated MSCs compared to osteoblasts, adipocytes, and chondrocytes at days 7 and 14 of differentiation. Additionally, IL-6 protein secretion levels measured by ELISA were greatly elevated in 7 day cultures of MSCs compared to MSCs that had been differentiated into osteoblasts (Figure 1B), showing that IL-6 mRNA transcript levels correlate with protein expression levels in MSCs.

IL-6 Induces Biologic Responses in MSCs

IL-6 Enhances Proliferation of Undifferentiated MSCs—To assess the role of IL-6 in undifferentiated MSC proliferation, we examined the effect of exogenous IL-6 on proliferation under serum-free conditions by MTT assay (data not shown) and direct cell counting. By both measures and across 3 patients, IL-6 significantly enhanced MSC proliferation after 1, 2, and 3 days in culture compared to untreated serum-free controls (Figure 2A).

Timing of IL-6-induced proliferation—*In vivo*, MSCs in the bone marrow reside in an IL-6 rich environment. Moreover, bone marrow-derived MSCs proliferate in relatively low levels of exogenous IL-6 [Ruster et al., 2006]. Therefore we wished to determine whether pre-treatment of MSCs with IL-6 could improve later proliferative capacity in IL-6-free conditions. MSCs were pre-treated for 48 h with 10 ng/mL IL-6 in serum-free medium, then placed in an IL-6-free environment and assessed for proliferation using the MTT assay. MSCs pre-treated with IL-6 showed a significant increase in proliferation compared to untreated controls at both 1 and 2 days following IL-6 removal (Figure 2B). This finding suggests that early IL-6 sensitization improves MSC proliferation and may play an important role in regulating their response to proliferative signals.

siRNA Knockdown of IL-6 Decreases Proliferation in MSCs

Given that exogenous IL-6 enhanced MSC proliferation, we next assessed whether endogenous IL-6 was also needed for MSC proliferation. *IL-6* gene expression was significantly inhibited by transfection with IL-6 siRNA relative to controls transfected with negative control siRNA (Figure 2C). Following transfection with siRNA targeting IL-6 mRNA, growth assessment revealed that loss of IL-6 expression was accompanied by significantly decreased MSC proliferation at both 2 and 3 days post-transfection, strongly suggesting that IL-6 plays a marked role in MSC proliferation (Figure 2D).

IL-6 Protects MSCs from Serum Starvation-Induced Apoptosis

To assess the effect of IL-6 on serum starvation-induced apoptosis of MSCs, undifferentiated MSCs were cultured under serum-free conditions for 72 h with or without IL-6 (10 ng/mL). Control cells had smaller, more pyknotic nuclei and brighter, more distinct TUNEL staining than MSCs serum-starved in the presence of IL-6 (Figure 3A). The average ratio of apoptotic cells in the absence *versus* presence of IL-6 was 3.5: 1 (Figure 3B), indicating that IL-6 protects MSCs from apoptosis induced by serum starvation. Additionally, IL-6 increased the overall cell density per well, consistent with the proliferation data described above.

To further analyze the mechanism by which IL-6 treatment delayed and/or decreased apoptosis after 72 h of serum starvation, we used pathway-based microarray tools to profile gene expression. IL-6-treated MSCs from 3 separate patients were compared to patient matched, serum-free controls. Using cut-off criteria, a 2.75-fold induction or repression of expression was considered to be of biologic importance. Fourteen genes were identified with greater than 2.75-fold repression of expression, consistent across all 3 patients (Figure 3C). Of these genes, *CD27* and *TRAF2* were significantly down-regulated.

IL-6 and Differentiation

IL-6 Inhibits Adipogenesis in MSCs—To assess the role of IL-6 in MSC differentiation down the adipogenic lineage, MSCs were induced to differentiate in adipogenesis induction medium with or without 10 ng/mL IL-6, and mRNA levels of the adipogenic markers *LPL* and *FABP4* were determined by real-time RT-PCR analysis. *LPL* gene expression was significantly reduced by IL-6 treatment (Figure 4A). Moreover, a similar trend was observed in *FABP4* gene expression (Figure 4B). Similarly, Oil Red O staining revealed both a qualitative and quantitative decrease in lipid droplet formation in MSCs differentiated in the presence of IL-6 (Figure 4C, D).

Time Course of IL-6 Suppression of Adipogenesis—The anti-adipogenic effects of IL-6 were next characterized by assessing whether IL-6 pre-treatment could effectively decrease MSC adipogenic differentiation. It should be noted that adipogenic differentiation, as described above, was carried out in differentiation medium for 21 days with serum, whereas the proliferation and apoptosis studies were done under serum-free conditions. The 3-week time course of differentiation precluded the use of serum-free culture conditions. The experimental design to assess early, rather than continuous IL-6 exposure allowed us to explore the effects of IL-6 both with and without serum. Early exposure was defined as 48 h of stimulation with IL-6, after which cells were allowed to differentiate in adipogenic medium in the absence of IL-6 for 18 days.

Early IL-6 exposure in serum-free medium prior to differentiation decreased mRNA transcript levels of *LPL* and *FABP4* (Figure 4E, F) at day 14. Early exposure to IL-6 in the presence of serum prior to differentiation did not alter *LPL* or *FABP4* expression across patients, possibly due to IL-6 binding and sequestration by serum proteins.

Effects of IL-6 on Osteogenic Differentiation—Cells were induced to differentiate in osteogenic medium in the absence or presence of 10 μg/ml IL-6. A statistically significant increase in *ALP* gene expression was observed at day 7 by real-time RT-PCR (Figure 5A). However, ALP histochemistry on day 10 showed equivalent staining intensity in the two groups (Figure 5C). Similarly, day 10 ALP activity assay revealed IL-6 exposure did not result in any reproducible trend across multiple patients (Figure 5D).

Day 18 Alizarin Red staining for calcium deposition revealed equivalent staining intensity in IL-6 treated cells (Figure 5C), and there is no significant quantitative difference in dye retention (Figure 5E). Real-time RT-PCR analysis of *OC* gene expression did not corroborate with the calcium deposition as indicated by Alizarin Red staining. By day 21 of differentiation, *OC* mRNA transcript levels were significantly decreased in IL-6 treated populations (Figure 5B).

Chondrogenesis—In a sample population (N=4 patients), MSC chondrogenic differentiation in the presence of IL-6 exhibited a statistically significant trend towards decreased *COL2A1* mRNA transcripts at day 21 (Figure 6A). Alcian blue staining for sulfated sGAG confirmed the chondro-inhibitory effect of IL-6 (Figure 6B). Concordantly, sGAG levels, as determined by the Blyscan assay, were significantly decreased by IL-6 treatment (Figure 6C). Furthermore, the larger size of IL-6-treated pellets (Figure 6B; quantification data not shown) was consistent with the mitogenic activity of IL-6 on MSCs.

In Vitro Wound Healing is Accelerated in the Presence of IL-6

As tissue-resident stem cells that can home to injury sites *in vivo*, MSCs are postulated to play an important role in wound healing [Francois et al., 2006; Ringden et al., 2007]. To assess the role of IL-6 in MSC-mediated acute wound healing, undifferentiated MSCs were injured in an *in vitro* model and defect closure following injury (cell migration) was monitored over 18 h in

a total of 30 defects (control, N=12; IL-6, N=18) using cells from two different patients. Cells treated with 10 ng/mL of IL-6 immediately following wounding showed an accelerated rate of wound closure compared to controls (Figure 7A). Quantitative analysis of these data revealed that IL-6 treatment results in a significant difference in the defect size at 6, 12, and 18 h post-injury compared to untreated controls (Figure 7B). The increased capacity for *in vitro* wound healing of IL-6-treated MSCs as early as 6 h in low-serum conditions indicates that IL-6 can induce MSC migration.

IL-6 Activates ERK1/2, but not STAT3 in MSCs

To assess the signaling pathway(s) through which IL-6 exerts its effects on human MSCs, we first explored whether IL-6 induces activation of the JAK/STAT pathway through phosphorylation of STAT3 at Tyr705 or Ser727, the mechanism commonly implicated in growth and proliferation of stem cell populations [Yoshida et al., 1994]. Stimulation with 10 ng/mL IL-6 for 60 min did not induce activation of STAT3 by phosphorylation at Tyr705 (Figure 8A) or Ser727 (data not shown). STAT3 was detected in all protein lysates, both experimental and control; however, only positive control cell lysates exhibited phospho-STAT3 expression at both Tyr705 (Figure 8A) and Ser727 (data not shown). STAT1 activation levels were also not affected by IL-6 treatment (data not shown).

To assess whether the ERK1/2 pathway is activated by IL-6 in MSCs, we stimulated MSCs with IL-6 and probed the cell lysates for total and phospho-ERK1/2. After 5 min of stimulation with IL-6, ERK1/2 phosphorylation could be detected. IL-6-mediated ERK1/2 activation peaked 30 min post IL-6-treatment before returning to baseline levels (Figure 8B). Therefore, in undifferentiated MSCs, IL-6 treatment activates ERK1/2 rather than STAT3.

Suppression of ERK1/2 Activation Inhibits IL-6-Mediated Increase in MSC Proliferation

To determine the importance of the ERK1/2 pathway, we blocked the activation of ERK1/2 with the MEK1/2 inhibitor U0126 prior to stimulation with IL-6 (Figure 8C). Following U0126-induced MEK1/2 inhibition, growth analysis revealed that reduced ERK1/2 signaling effectively inhibited IL-6-mediated enhancement of MSC proliferation (Figure 8D). These data suggest that signaling via the ERK1/2 pathway is critical for IL-6-mediated proliferation of MSCs.

IL-6 Inhibition of MSC Differentiation is Reversed in the Presence of U0126

We next examined the involvement of ERK1/2 signaling in IL-6-induced inhibition of adipogenic differentiation by using U0126. Prior to differentiation, MSCs were expanded for 72 h with or without IL-6 and/or U0126, and then grown in adipogenic medium for 18 days.

The IL-6-mediated decrease in adipogenic mRNA transcripts previously observed at day 14 for *LPL* and *FABP4* was abrogated by exposure to U0126 (Figure 8E, F). The IL-6 effect on chondrogenesis was also dependent on ERK1/2 activation. Specifically, the IL-6-mediated decrease in *COL2A1* expression was abrogated by co-treatment with U0126 (Figure 8G). These data suggest that signaling via the ERK1/2 pathway is critical for IL-6-mediated stem cell maintenance.

DISCUSSION

We have recently shown that *IL-6* expression is down-regulated as MSCs undergo mesenchymal differentiation, and that this expression resumes its undifferentiated levels upon dedifferentiation from adipogenic and chondrogenic lineages [Song et al., 2006]. We chose to pursue IL-6 as a candidate “stemness” gene for a number of reasons. IL-6 and IL-6 type cytokines have been shown to activate the JAK/STAT, MAPK, and AKT pathways and have

been implicated as potent mediators of numerous important biological processes, including differentiation, proliferation, and apoptosis [Heinrich et al., 1998]. In stem cell biology, IL-6 family cytokines have been implemented in the maintenance of both embryonic and adult stem cells. IL-6 increases proliferation in placenta-derived MSCs [Li et al., 2007] and is highly expressed in cord blood [Liu and Hwang, 2005] and bone marrow-derived MSCs [Rougier et al., 1998]. Oncostatin M, an IL-6 type cytokine, induces proliferation [Song et al., 2005], increases osteogenesis and inhibits adipogenesis [Gimble et al., 1994; Song et al., 2007] in adipose-derived MSCs. IL-6 is also integral to normal stromal cell function and osteoclast activation [Manolagas and Jilka, 1995] and both hemato- and myelopoiesis [Bernad et al., 1994; Ikebuchi et al., 1987; Ishibashi et al., 1989]. Moreover, liver regeneration *in vivo* involves IL-6, as IL-6 knockout mice have impaired liver regeneration and fail to repair ischemia/reperfusion injury, a defect that is correctable by addition of exogenous IL-6 [Camargo et al., 1997; Cressman et al., 1996]. Our data reported here show, for the first time, that IL-6 maintains the “stemness” of bone marrow-derived MSCs. Specifically, IL-6 enhances proliferation and protects from serum starvation-induced apoptosis of undifferentiated MSCs. Furthermore, IL-6 inhibits adipogenic and chondrogenic differentiation, and increases the rate of *in vitro* wound healing of MSCs.

In this study, we show that IL-6 induces ERK1/2 activation in undifferentiated MSCs but not STAT3, the downstream regulator of the gp130/IL-6 family signaling pathway. Furthermore, ERK1/2 pathway inhibition mitigates the IL-6 effects, resulting in decreased proliferation and increased differentiation along both the adipogenic and chondrogenic lineages. Osteogenesis was not affected by IL-6 exposure, suggesting different transcriptional regulation. A balance between ERK1/2 and STAT3 activation, in terms of signal transduction, has been described in many cell types. Mouse ES cells express IL-6, gp130 receptors, and other members of the IL-6 cytokine family, and the “stemness” of these cells can be maintained by activation of the JAK/STAT pathway [Nichols et al., 1994; Yoshida et al., 1994]. Human ES cells express these same cytokines and receptors; however, loss of the pluripotency markers Nanog and Oct-4 occurs despite signaling through gp130 pathways [Humphrey et al., 2004]. In fact, despite similar marked activation of both ERK1/2 and STAT3, different effects on “stemness” were observed in human and mouse ES cells. Our results show that, although IL-6 maintains MSC “stemness”, it does not activate the JAK/STAT pathway. This is distinct from the balance between STAT3 (pluripotent) and ERK1/2 (loss of pluripotency) activity previously described in ES cells, and suggests a novel signaling mechanism in MSCs [Burdon et al., 2002; Smith, 2001].

It has been demonstrated that p38 MAPK is a critical regulator of IL-6 production in human thymic epithelial cells [Mainiero et al., 2003]. Accordingly, p38 may be involved in the gene expression of IL-6; however it is unknown if p38, or JNK for that matter, are critical for IL-6 mediated cell proliferation and survival, particularly in MSCs. We did not test if JNK or p38 are activated in response to IL-6 in MSCs. It is possible that p38 may be important for MSC proliferation since it has been shown to play an important role in IL-6 mediated proliferation of B9 hybridoma cells [Zauberman et al., 1999]. However, in contrast to our findings in MSCs, that study did not find induction of ERK1/2 in response to IL-6 treatment. So it appears that the involvement of particular MAP kinases in IL-6 mediated proliferation and survival is highly cell type specific. The unique role of IL-6-induced ERK1/2 activation in MSCs may be due to a signature profile of the ligand-specific cell surface receptors. This signature has yet to be defined for MSCs.

Of further interest is the mechanism by which IL-6 appears to mitigate apoptotic pathways in MSCs. The down- regulated gene profile in our PCR array includes genes involved in NFκB-mediated apoptosis, certain immunoregulatory factors, as well as elements of the intrinsic apoptotic pathway. For example, of the down-regulated genes in our experimental system

TRAF2 is known to interact with TNFRII, CD40 [Hu et al., 1994] as well as CD27 [Akiba et al., 1998] amongst other regulators of apoptosis, and its over-expression can induce NFκB activation [Rothe et al., 1995]. Similarly, CD27 signaling activates NFκB and JNK/SAPK through a TRAF2 dependent mechanism [Akiba et al., 1998]. Additionally, the down-regulation of caspases 9 and 6 are of interest because caspase 9 is an important initiator of intrinsic apoptosis [Li et al., 1997], and caspase 6 is an effector caspase shown to inhibit caspase 9 signaling [Guerrero et al., 2008]. The significance of other down-regulated genes is more ambiguous, such as anti-apoptotic BCL2L10 and NAIP and pro-apoptotic BID and BAK1, mediators of the intrinsic apoptotic pathway [Cory et al., 2003].

In the adult stem cell field, it is unknown whether MSCs regenerate tissue directly or act via their byproducts to re-invigorate other adult tissue-resident stem cells. Preliminary data from our laboratory suggest that IL-6 is one of the MSC products functioning to re-invigorate tissue. Specifically, the addition of exogenous, recombinant IL-6 to MSC cultures stimulated endogenous IL-6 gene expression in MSCs (data not shown). Based on these initial data, we speculate that exogenous IL-6 may form a positive autocrine feedback loop in MSCs, perhaps functioning to augment the proliferative signal to neighboring MSCs. Our results show an important role for IL-6 in MSC maintenance and functionality. We believe IL-6 is necessary not only for maintenance of MSCs in their stem state and niche, but also for their support of the hematopoietic stem cells with which they interact in the bone marrow microenvironment. IL-6 has long been known to play an integral role in normal hematopoiesis and myelopoiesis, and it is thus particularly interesting that IL-6 would also play a prominent role in the maintenance of MSCs. The inhibition of stromal adipogenesis by IL-6 is directly relevant for homeostasis of the bone marrow niche and is most likely a key mechanism by which co-infusion of MSC and HSCs results in more efficient reconstitution of the bone marrow following bone marrow transplantation [Koc et al., 2000].

In summary, we have shown here, for the first time, that IL-6 is a critical factor for maintaining the stemness of adult human bone marrow-derived MSCs. This finding is important for understanding the regulation of MSCs by their microenvironment, as well as optimizing the manipulation of these cells *in vitro* and *in vivo*.

Acknowledgments

Contract grant sponsor: Intramural Research Program of NIAMS, NIH

Contract grant number: Z01 AR41131

We thank Dr. Brent Bobick (NIH/NIAMS/CBOB) for critical reading of this manuscript. We would also like to thank Dr. Kristien Zaal (NIH/NIAMS/Light Imaging Section) for technical support with microscopy. Financial support: Intramural Research Program of NIAMS, NIH (Z01 AR41137); KLP is a Research Scholar in the HHMI-NIH Research Scholars Program.

References

Akiba H, Nakano H, Nishinaka S, Shindo M, Kobata T, Atsuta M, Morimoto C, Ware CF, Malinin NL, Wallach D, Yagita H, Okumura K. CD27, a member of the tumor necrosis factor receptor superfamily, activates NF-kappaB and stress-activated protein kinase/c-Jun N-terminal kinase via TRAF2, TRAF5, and NF-kappaB-inducing kinase. J Biol Chem 1998;273:13353–8. [PubMed: 9582383]

Bernad A, Kopf M, Kulbacki R, Weich N, Koehler G, Gutierrez-Ramos JC. Interleukin-6 is required in vivo for the regulation of stem cells and committed progenitors of the hematopoietic system. Immunity 1994;1:725–31. [PubMed: 7895162]

Burdon T, Smith A, Savatier P. Signalling, cell cycle and pluripotency in embryonic stem cells. Trends Cell Biol 2002;12:432–8. [PubMed: 12220864]

Camargo CA Jr, Madden JF, Gao W, Selvan RS, Clavien PA. Interleukin-6 protects liver against warm ischemia/reperfusion injury and promotes hepatocyte proliferation in the rodent. Hepatology 1997;26:1513–20. [PubMed: 9397992]

Conget PA, Minguell JJ. Phenotypical and functional properties of human bone marrow mesenchymal progenitor cells. J Cell Physiol 1999;181:67–73. [PubMed: 10457354]

Cory S, Huang DC, Adams JM. The Bcl-2 family: roles in cell survival and oncogenesis. Oncogene 2003;22:8590–607. [PubMed: 14634621]

Cressman DE, Greenbaum LE, DeAngelis RA, Ciliberto G, Furth EE, Poli V, Taub R. Liver failure and defective hepatocyte regeneration in interleukin-6-deficient mice. Science 1996;274:1379–83. [PubMed: 8910279]

Francois S, Bensidhoum M, Mouiseddine M, Mazurier C, Allenet B, Semont A, Frick J, Sache A, Bouchet S, Thierry D, Gourmelon P, Gorin NC, Chapel A. Local irradiation not only induces homing of human mesenchymal stem cells at exposed sites but promotes their widespread engraftment to multiple organs: a study of their quantitative distribution after irradiation damage. Stem Cells 2006;24:1020–9. [PubMed: 16339642]

Gimble JM, Wanker F, Wang CS, Bass H, Wu X, Kelly K, Yancopoulos GD, Hill MR. Regulation of bone marrow stromal cell differentiation by cytokines whose receptors share the gp130 protein. J Cell Biochem 1994;54:122–33. [PubMed: 8126083]

Guerrero AD, Chen M, Wang J. Delineation of the caspase-9 signaling cascade. Apoptosis 2008;13:177–86. [PubMed: 17899380]

Heinrich PC, Behrmann I, Muller-Newen G, Schaper F, Graeve L. Interleukin-6-type cytokine signalling through the gp130/Jak/STAT pathway. Biochem J 1998;334(Pt 2):297–314. [PubMed: 9716487]

Hu HM, O'Rourke K, Boguski MS, Dixit VM. A novel RING finger protein interacts with the cytoplasmic domain of CD40. J Biol Chem 1994;269:30069–72. [PubMed: 7527023]

Humphrey RK, Beattie GM, Lopez AD, Bucay N, King CC, Firpo MT, Rose-John S, Hayek A. Maintenance of pluripotency in human embryonic stem cells is STAT3 independent. Stem Cells 2004;22:522–30. [PubMed: 15277698]

Ikebuchi K, Wong GG, Clark SC, Ihle JN, Hirai Y, Ogawa M. Interleukin 6 enhancement of interleukin 3-dependent proliferation of multipotential hemopoietic progenitors. Proc Natl Acad Sci U S A 1987;84:9035–9. [PubMed: 3501121]

Ishibashi T, Kimura H, Uchida T, Kariyone S, Friese P, Burstein SA. Human interleukin 6 is a direct promoter of maturation of megakaryocytes in vitro. Proc Natl Acad Sci U S A 1989;86:5953–7. [PubMed: 2788282]

Jiang Y, Jahagirdar BN, Reinhardt RL, Schwartz RE, Keene CD, Ortiz-Gonzalez XR, Reyes M, Lenvik T, Lund T, Blackstad M, Du J, Aldrich S, Lisberg A, Low WC, Largaespada DA, Verfaillie CM. Pluripotency of mesenchymal stem cells derived from adult marrow. Nature 2002;418:41–9. [PubMed: 12077603]

Koc ON, Gerson SL, Cooper BW, Dyhouse SM, Haynesworth SE, Caplan AI, Lazarus HM. Rapid hematopoietic recovery after coinfusion of autologous-blood stem cells and culture-expanded marrow mesenchymal stem cells in advanced breast cancer patients receiving high-dose chemotherapy. J Clin Oncol 2000;18:307–16. [PubMed: 10637244]

Le Blanc K, Gotherstrom C, Ringden O, Hassan M, McMahon R, Horwitz E, Anneren G, Axelsson O, Nunn J, Ewald U, Norden-Lindeberg S, Jansson M, Dalton A, Astrom E, Westgren M. Fetal mesenchymal stem-cell engraftment in bone after in utero transplantation in a patient with severe osteogenesis imperfecta. Transplantation 2005;79:1607–14. [PubMed: 15940052]

Le Blanc K, Rasmusson I, Sundberg B, Gotherstrom C, Hassan M, Uzunel M, Ringden O. Treatment of severe acute graft-versus-host disease with third party haploidentical mesenchymal stem cells. Lancet 2004;363:1439–41. [PubMed: 15121408]

Li D, Wang GY, Dong BH, Zhang YC, Wang YX, Sun BC. Biological characteristics of human placental mesenchymal stem cells and their proliferative response to various cytokines. Cells Tissues Organs 2007;186:169–79. [PubMed: 17630477]

Li P, Nijhawan D, Budihardjo I, Srinivasula SM, Ahmad M, Alnemri ES, Wang X. Cytochrome c and dATP-dependent formation of Apaf-1/caspase-9 complex initiates an apoptotic protease cascade. Cell 1997;91:479–89. [PubMed: 9390557]

Liu CH, Hwang SM. Cytokine interactions in mesenchymal stem cells from cord blood. Cytokine 2005;32:270–9. [PubMed: 16377203]

Mainiero F, Colombara M, Antonini V, Strippoli R, Merola M, Poffe O, Tridente G, Ramarli D. p38 MAPK is a critical regulator of the constitutive and the beta4 integrin-regulated expression of IL-6 in human normal thymic epithelial cells. Eur J Immunol 2003;33:3038–48. [PubMed: 14579272]

Manolagas SC. Role of cytokines in bone resorption. Bone 1995;17:63S–67S. [PubMed: 8579900]

Manolagas SC, Jilka RL. Bone marrow, cytokines, and bone remodeling. Emerging insights into the pathophysiology of osteoporosis. N Engl J Med 1995;332:305–11. [PubMed: 7816067]

Nesti LJ, Jackson WM, Shanti RM, Koehler SM, Aragon AB, Bailey JR, Sracic MK, Freedman BA, Giuliani JR, Tuan RS. Differentiation potential of multipotent progenitor cells derived from war-traumatized muscle tissue. J Bone Joint Surg Am 2008;90:2390–8. [PubMed: 18978407]

Nichols J, Chambers I, Smith A. Derivation of germline competent embryonic stem cells with a combination of interleukin-6 and soluble interleukin-6 receptor. Exp Cell Res 1994;215:237–9. [PubMed: 7957676]

Ogasawara H, Tsuji T, Hirano D, Aoki Y, Nakamura M, Kodama H. Induction of IL-6 production by bone marrow stromal cells on the adhesion of IL-6-dependent hematopoietic cells. J Cell Physiol 1996;169:209–16. [PubMed: 8841437]

Pereira RF, Halford KW, O'Hara MD, Leeper DB, Sokolov BP, Pollard MD, Bagasra O, Prockop DJ. Cultured adherent cells from marrow can serve as long-lasting precursor cells for bone, cartilage, and lung in irradiated mice. Proc Natl Acad Sci U S A 1995;92:4857–61. [PubMed: 7761413]

Pittenger MF, Mackay AM, Beck SC, Jaiswal RK, Douglas R, Mosca JD, Moorman MA, Simonetti DW, Craig S, Marshak DR. Multilineage potential of adult human mesenchymal stem cells. Science 1999;284:143–7. [PubMed: 10102814]

Prockop DJ. Marrow stromal cells as stem cells for nonhematopoietic tissues. Science 1997;276:71–4. [PubMed: 9082988]

Ringden O, Uzunel M, Sundberg B, Lonnies L, Nava S, Gustafsson J, Henningsohn L, Le Blanc K. Tissue repair using allogeneic mesenchymal stem cells for hemorrhagic cystitis, pneumomediastinum and perforated colon. Leukemia 2007;21:2271–6. [PubMed: 17611560]

Rothe M, Sarma V, Dixit VM, Goeddel DV. TRAF2-mediated activation of NF-kappa B by TNF receptor 2 and CD40. Science 1995;269:1424–7. [PubMed: 7544915]

Rougier F, Cornu E, Praloran V, Denizot Y. IL-6 and IL-8 production by human bone marrow stromal cells. Cytokine 1998;10:93–7. [PubMed: 9512898]

Ruster B, Gottig S, Ludwig RJ, Bistrian R, Muller S, Seifried E, Gille J, Henschler R. Mesenchymal stem cells display coordinated rolling and adhesion behavior on endothelial cells. Blood 2006;108:3938–44. [PubMed: 16896152]

Sarugaser R, Lickorish D, Baksh D, Hosseini MM, Davies JE. Human umbilical cord perivascular (HUCPV) cells: a source of mesenchymal progenitors. Stem Cells 2005;23:220–9. [PubMed: 15671145]

Seck T, Diel I, Bismar H, Ziegler R, Pfeilschifter J. Expression of Interleukin-6 (IL-6) and IL-6 receptor mRNA in human bone samples from pre- and postmenopausal women. Bone 2002;30:217–22. [PubMed: 11792588]

Smith AG. Embryo-derived stem cells: of mice and men. Annu Rev Cell Dev Biol 2001;17:435–62. [PubMed: 11687496]

Song HY, Jeon ES, Jung JS, Kim JH. Oncostatin M induces proliferation of human adipose tissue-derived mesenchymal stem cells. Int J Biochem Cell Biol 2005;37:2357–65. [PubMed: 15979922]

Song HY, Jeon ES, Kim JI, Jung JS, Kim JH. Oncostatin M promotes osteogenesis and suppresses adipogenic differentiation of human adipose tissue-derived mesenchymal stem cells. J Cell Biochem 2007;101:1238–51. [PubMed: 17226768]

Song L, Tuan RS. Transdifferentiation potential of human mesenchymal stem cells derived from bone marrow. FASEB J 2004;18:980–2. [PubMed: 15084518]

Song L, Webb NE, Song Y, Tuan RS. Identification and functional analysis of candidate genes regulating mesenchymal stem cell self-renewal and multipotency. Stem Cells 2006;24:1707–18. [PubMed: 16574750]

Yoshida K, Chambers I, Nichols J, Smith A, Saito M, Yasukawa K, Shoyab M, Taga T, Kishimoto T. Maintenance of the pluripotential phenotype of embryonic stem cells through direct activation of gp130 signalling pathways. Mech Dev 1994;45:163–71. [PubMed: 8199053]

Zauberman A, Zipori D, Krupsky M, Ben-Levy R. Stress activated protein kinase p38 is involved in IL-6 induced transcriptional activation of STAT3. Oncogene 1999;18:3886–93. [PubMed: 10445852]

Zuk PA, Zhu M, Ashjian P, De Ugarte DA, Huang JI, Mizuno H, Alfonso ZC, Fraser JK, Benhaim P, Hedrick MH. Human adipose tissue is a source of multipotent stem cells. Mol Biol Cell 2002;13:4279–95. [PubMed: 12475952]

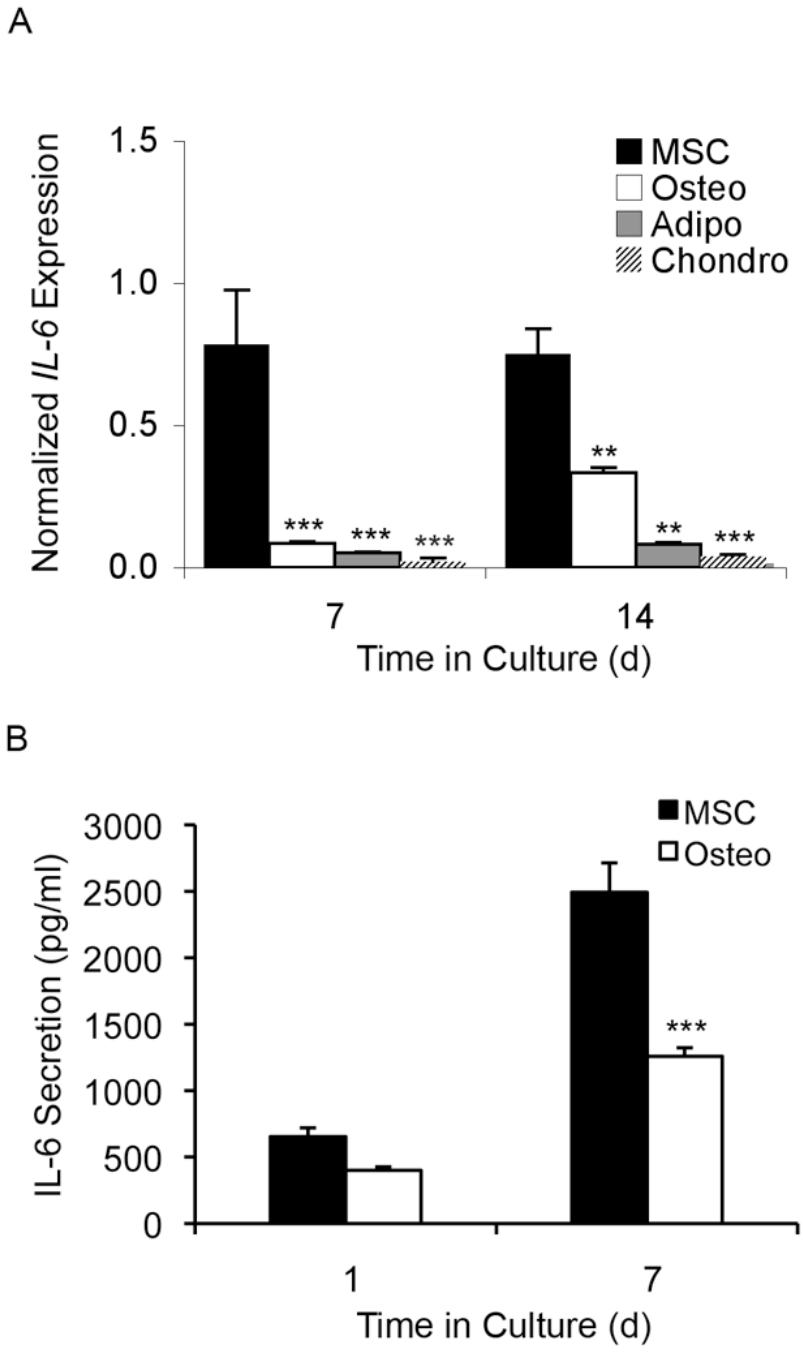

Figure 1. *IL-6* gene expression is significantly lower in differentiated vs. undifferentiated MSCs

(A) Graph showing *IL-6* gene expression of undifferentiated MSCs (MSC) and MSCs that have undergone osteogenic (Osteo), adipogenic (Adipo), and chondrogenic (Chondro) differentiation. Data are normalized against *GAPDH*. Compared to undifferentiated MSCs, *IL-6* mRNA levels were 5-fold and 2-fold lower in osteogenic cells at days 7 and 14 of differentiation; 9-fold and 3-fold lower in adipogenic cells at day 7 and day 14 of differentiation; and 18-fold and 20-fold lower in chondrogenic cells at day 7 and day 14 of differentiation (ANOVA, all compared to MSC: * $p < 0.05$, ** $p < 0.01$, *** $p < 0.001$). **(B)** Graph showing IL-6 protein secretion levels as measured by ELISA for undifferentiated MSCs and osteogenic differentiated MSCs. After 7 days of osteogenic differentiation, there was a

significant 2-fold drop in IL-6 secretion levels compared to undifferentiated MSC controls (t-test: *** $p < 0.001$).

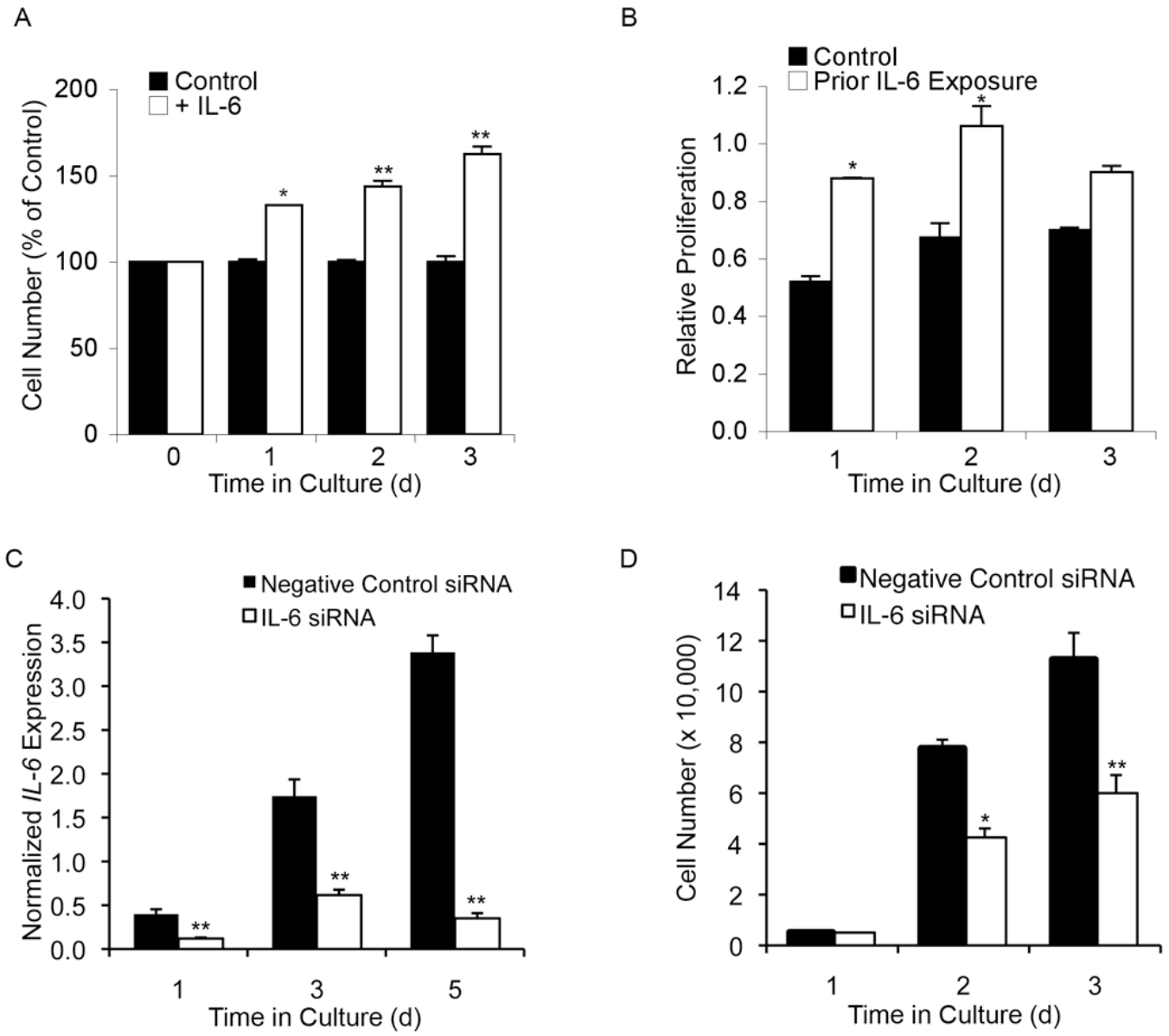

Figure 2. IL-6 enhances proliferation of undifferentiated MSCs

(A) Compared to non-stimulated controls, undifferentiated MSCs grown in the presence of IL-6 (10 ng/mL) had a 32% ± 3, 44% ± 8, and 62% ± 14 increase in cell number after 1, 2, and 3 days of growth, respectively. **(B)** Graph showing results from the MTT assay. Compared to non-stimulated controls, undifferentiated MSCs previously maintained in an IL-6 rich environment proliferated at a higher rate up to 2 days following removal of IL-6 stimulation. **(C)** Following siRNA knockdown**,** real-time RT-PCR analysis of *IL-6* transcript levels revealed an average 60% 90% decrease in *IL-6* expression compared to transfected controls up to 5 days post transfection. **(D)** Loss of IL-6 expression decreased MSC proliferation by almost 50% at both 2 and 3 days post-transfection. A-D: Student's t-test analysis, * $p < 0.05$, ** $p < 0.01$.

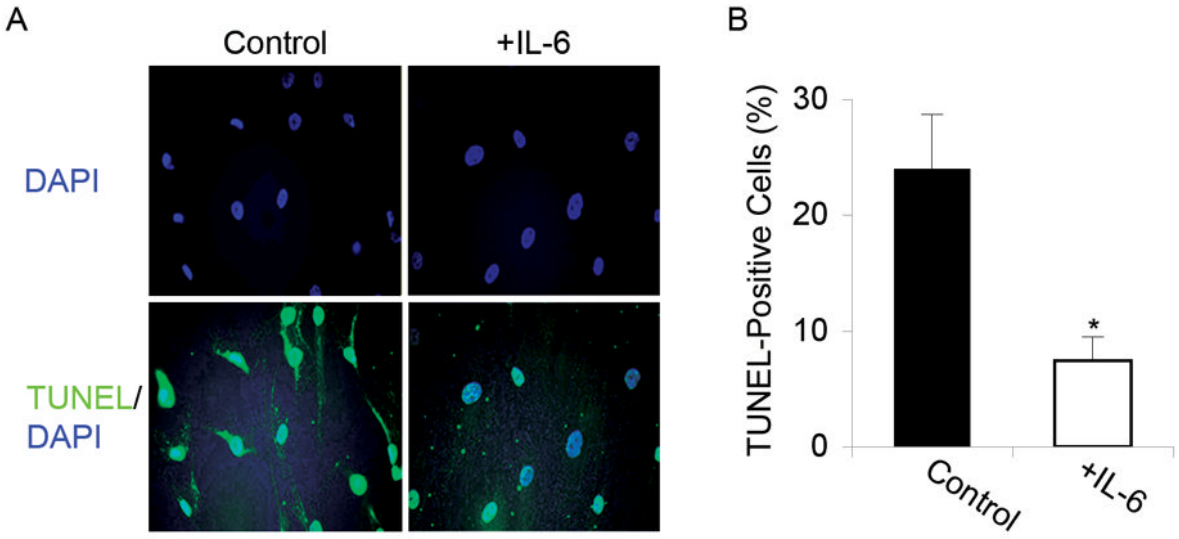

C

IL-6 Treated vs Control Group @ 72hr			
Gene Symbol	Fold Change	Fold Down-Regulation	p-value
BAK1	0.3268	-3.06	0.303
BCL2L10	0.3503	-2.85	0.145
BFAR	0.3121	-3.2	0.213
BID	0.298	-3.36	0.265
NAIP	0.3345	-2.99	0.146
BNIP3L	0.3194	-3.13	0.225
CASP6	0.3423	-2.92	0.185
CASP9	0.242	-4.13	0.146
CD40	0.2594	-3.85	0.163
TNFRSF10A	0.2535	-3.94	0.107
TNFRSF10B	0.3423	-2.92	0.186
CD27*	0.1525	-6.56	**0.039**
CD70	0.305	-3.28	0.305
TRAF2*	0.3503	-2.85	**0.037**

Figure 3. IL-6 protects MSCs from serum starvation-induced apoptosis

(A) TUNEL: Apoptosis was evaluated using TUNEL staining in undifferentiated MSCs grown in serum-free media for 72 h with or without IL-6. IL-6 treated populations exhibited fewer apoptotic cells compared to untreated controls. DAPI staining revealed IL-6 treated cells had smaller, more pyknotic nuclei and TUNEL staining was more intense in MSCs serum-starved and treated with IL-6. Magnification: 20X. **(B) Cell counts:** For each condition**,** total numbers of TUNEL-positive cells were counted and a ratio of the means was calculated. The mean ratio of apoptotic cells in serum-free conditions to apoptotic cells in IL-6 supplemented conditions was 3.5: 1 (t-test: * $p < 0.05$). **(C) Microarray gene expression analysis:** Expression levels

of pro-apoptotic genes decreased upon treatment with IL-6 for 72 h, only significantly for *CD27* and *TRAF2*.

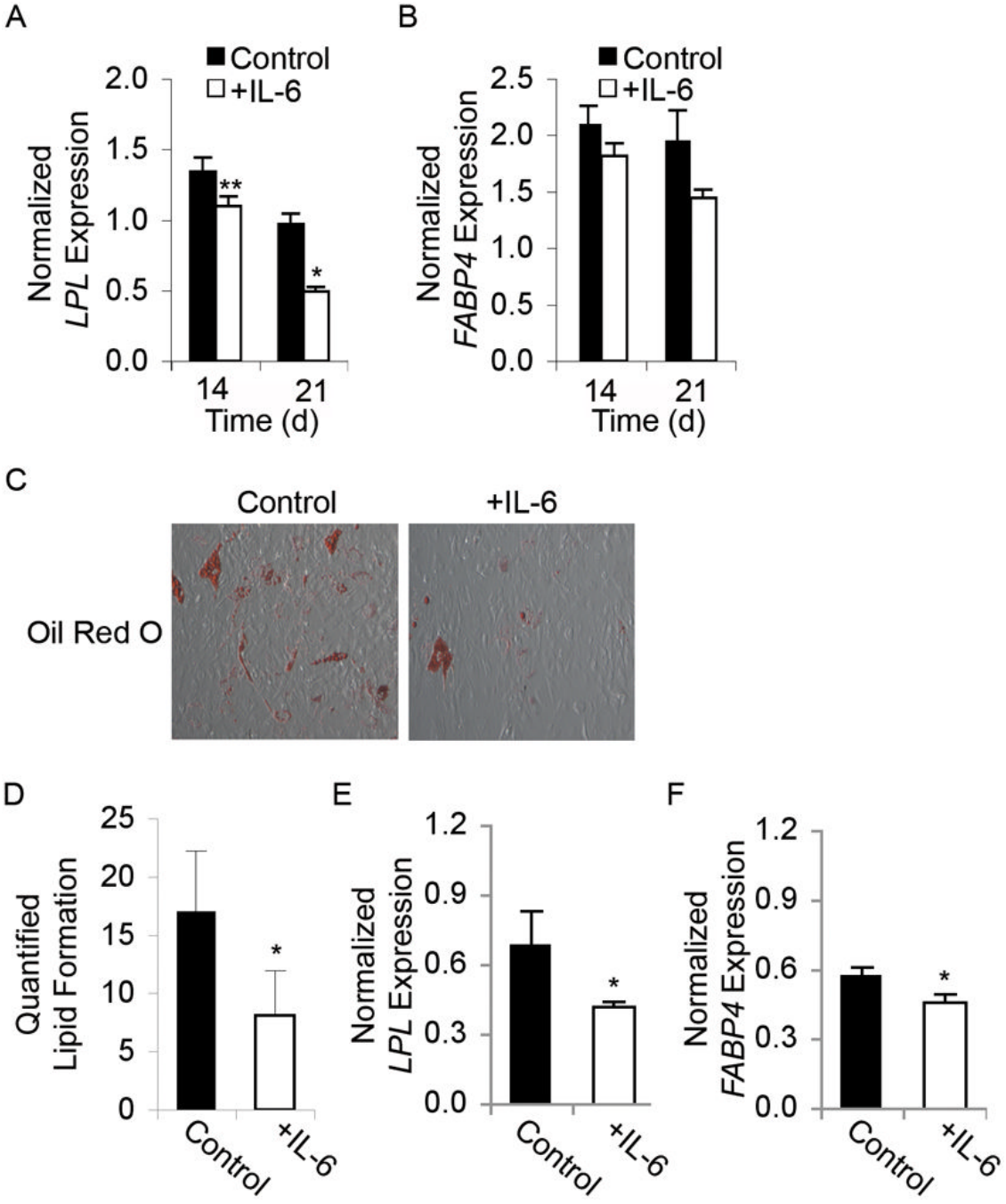

Figure 4. IL-6 inhibits adipogenic differentiation of MSCs

(A) Graph showing real-time RT-PCR results of *LPL* and **(B)** *FABP4* gene expression normalized to *GAPDH* in MSCs induced to undergo adipogenesis without (Control) or with IL-6 treatment for 14 or 21 days. In adipocytes differentiated in the presence of IL-6, *LPL* expression decreased by 20% at day 14 and 50% by day 21, and *FABP4* gene expression decreased by 20% at day 21 (N=3). **(C)** Oil Red O staining is shown to reveal the presence of lipid droplets, indicating adipogenic differentiation. Images were taken at 20x magnification. **(D)** Graph showing quantification of Oil Red O staining, which reveals that IL-6 treatment significantly decreased lipidization. **(E)** Graph showing real-time RT-PCR results of *LPL* and **(F)** *FABP4* gene expression normalized to *GAPDH* in MSCs pre-treated with IL-6 for 48 h

prior to adipogenic differentiation for 18 d. A, D-F: Student's t-test analysis, * $p < 0.05$, ** $p < 0.01$.

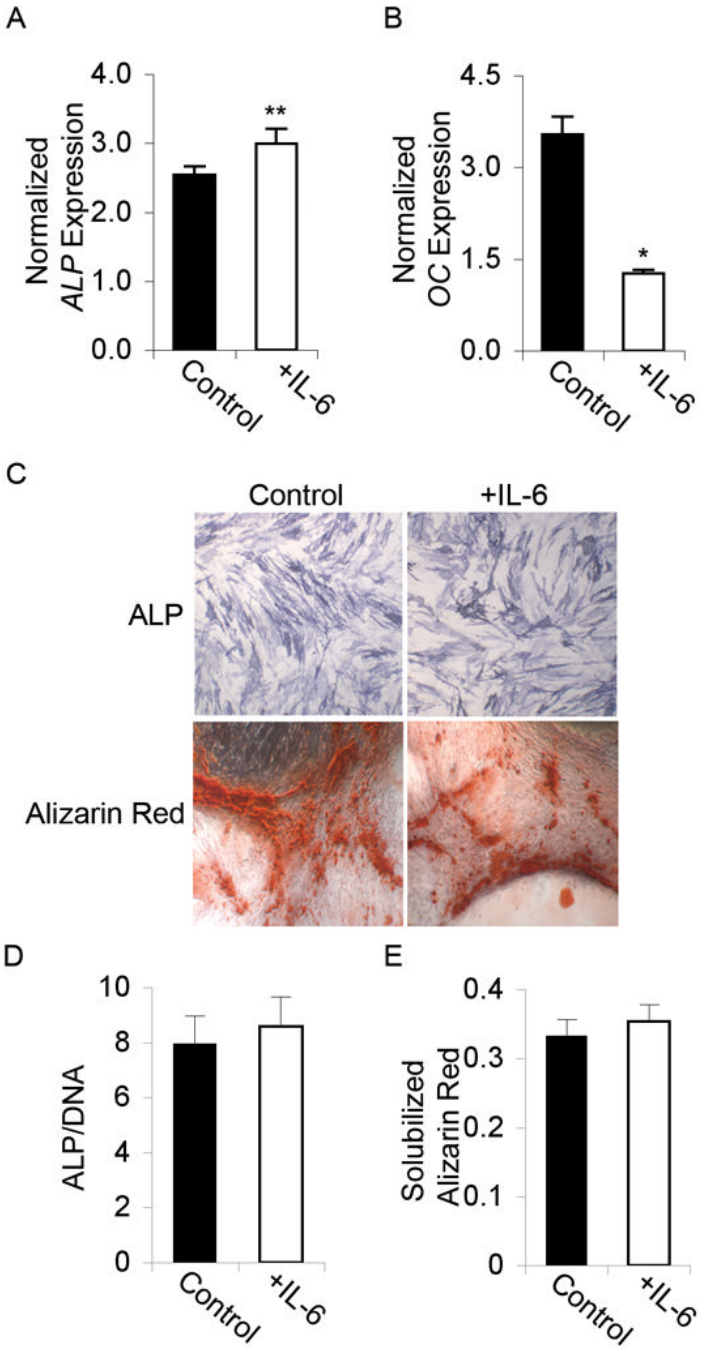

Figure 5. IL-6 does not affect osteogenic differentiation of MSCs

(A) Graph showing real-time RT-PCR results of Alkaline Phosphatase (*ALP*) gene expression at day 7 and **(B)** Osteocalcin (*OC*) gene expression at day 21, both normalized to *GAPDH* in MSCs induced to undergo osteogenesis without (Control) or with IL-6 treatment. A, B: Student's t-test analysis, * $p < 0.05$, ** $p < 0.01$. **(C)** Immunohistochemical staining of ALP and Alizarin Red, both showing no difference between Control and +IL-6 treated cells. Images were taken at 4x magnification. **(D)** ALP activity assay results of osteogenic differentiated MSCs in the absence (Control) or presence of IL-6. Data are normalized to total DNA content. **(E)** Graph showing quantification of Alizarin Red staining.

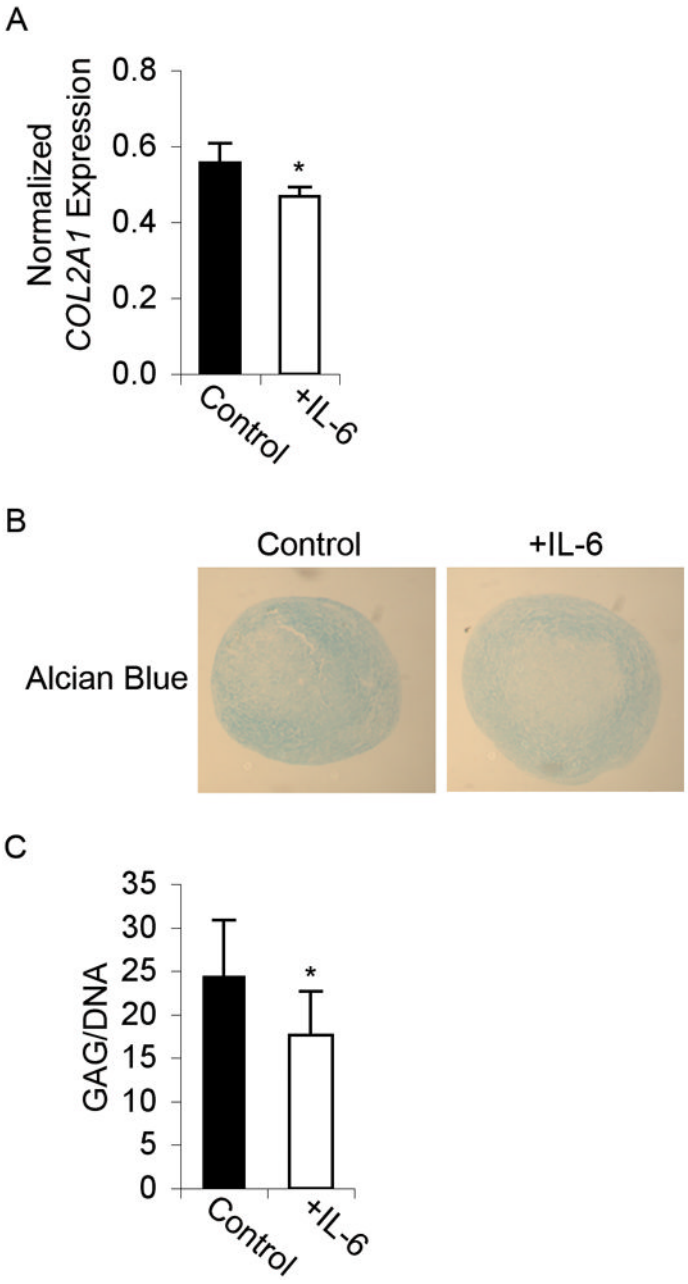

Figure 6. IL-6 treatment suppresses chondrogenic differentiation of MSCs

(A) Graph showing real-time RT-PCR results of Collagen II (*COL2A1*) gene expression normalized to *GAPDH* at day 21 of differentiation in MSCs induced to undergo chondrogenesis without (Control) or with IL-6 treatment (N=4). **(B)** Alcian Blue immunohistochemical staining, showing decreased glycosaminoglycan expression in chondrogenic-differentiated pellets treated with IL-6. Images were taken at 4x magnification. **(C)** Consistent with the qualitative observations above, the sGAG assay results show a significant decrease in sulfated glycosaminoglycan formation in chondrogenic-differentiated MSCs treated with IL-6 for 21 days. Data are normalized to total DNA content. A, C: Student's t-test analysis, * $p < 0.05$.

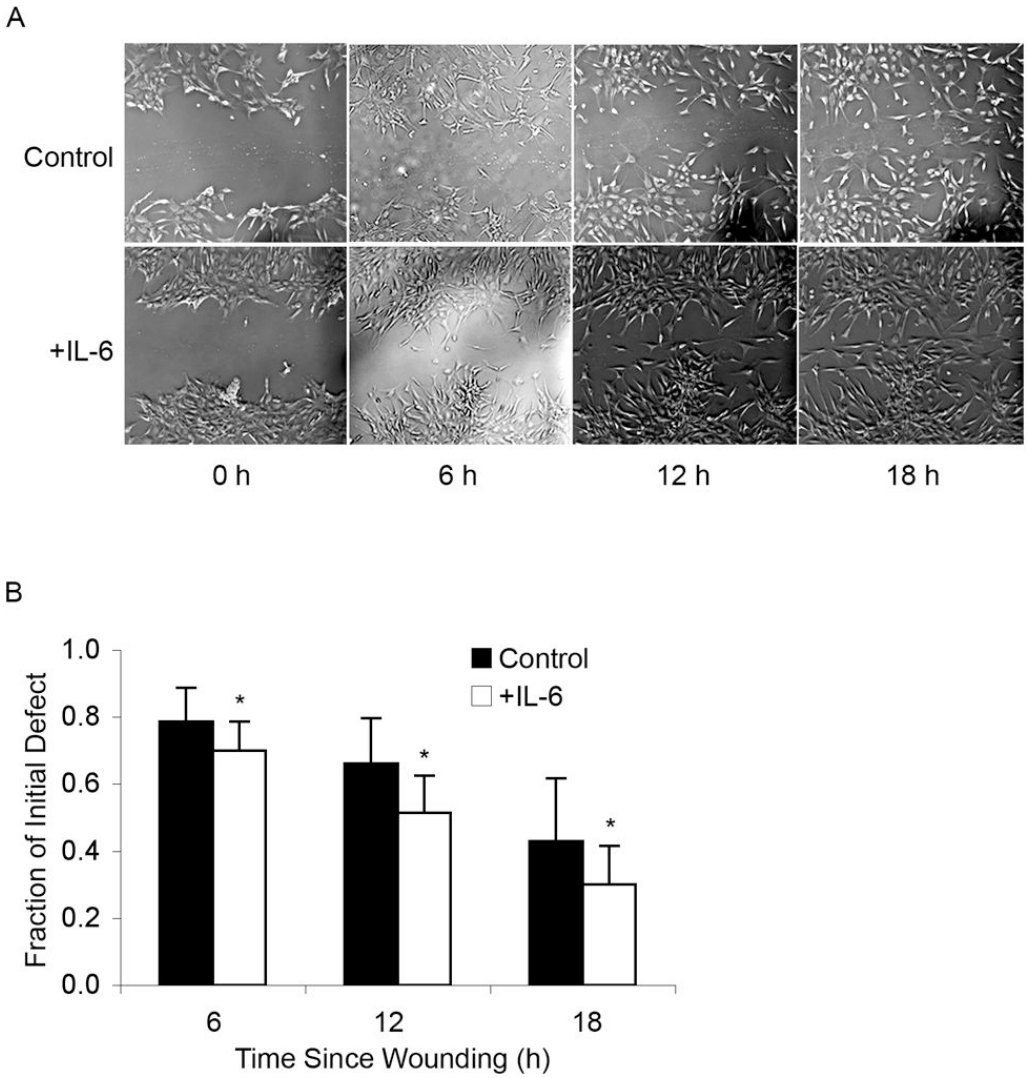

Figure 7. IL-6 accelerates *in vitro* wound healing in MSCs

(A) Wound healing: Confluent, undifferentiated MSCs were wounded and defect closure was observed over 18 h either in the absence (Control) or presence of IL-6. Defects were imaged at the time of wounding (0 h) and then at 6 h intervals for 18 h. MSCs exposed to IL-6 after initial wounding showed increased capacity for *in vitro* healing. Images were taken at 5x magnification. **(B) Quantitative analysis:** The remaining wound area in the presence of IL-6 at 6 h post-injury was approximately 15% less than that of untreated MSCs, at 12 h post-injury was approximately 33% less than untreated MSCs, and at 18 h was approximately 24% less than untreated MSCs (t-test: * $p < 0.05$).

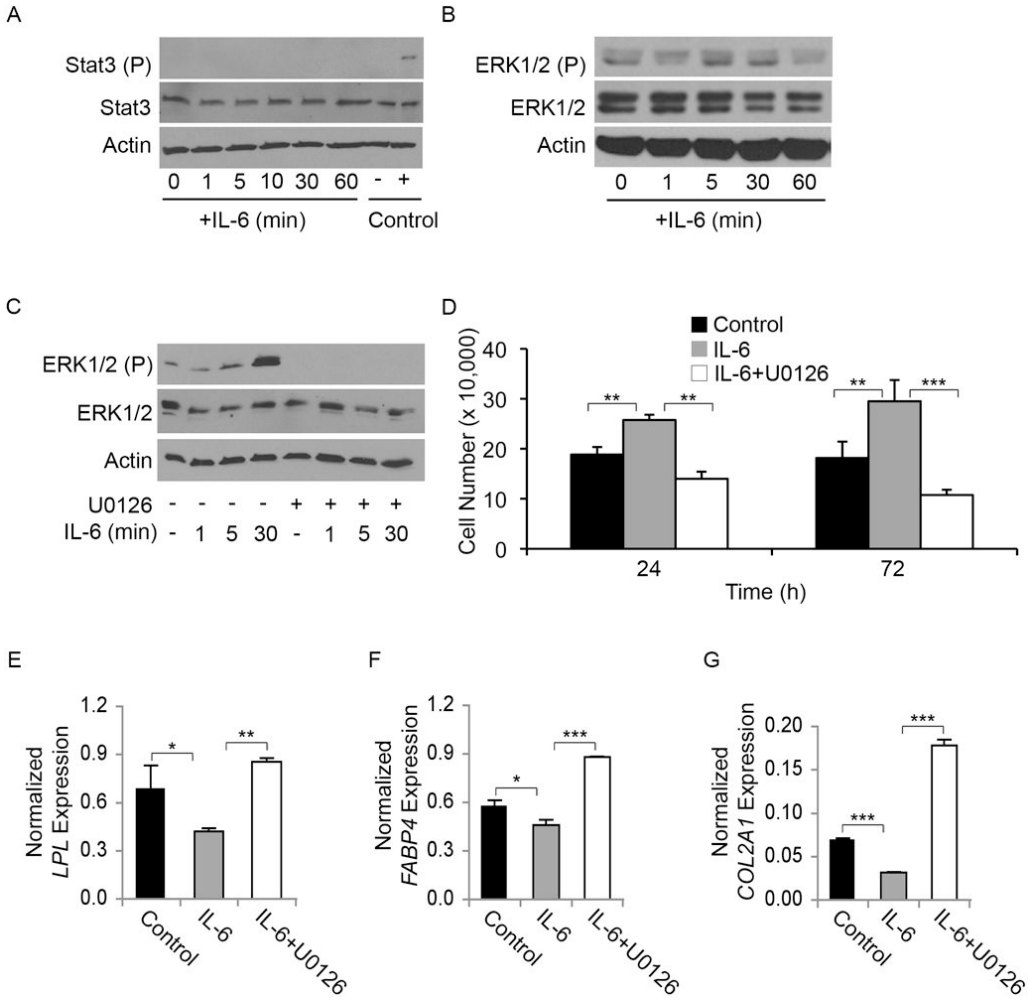

Figure 8. IL-6 mediated effects in MSCs are dependent upon ERK1/2 activation

Undifferentiated MSCs were serum-starved for 12 h and then stimulated with IL-6 (10 ng/mL) for 0–60 min. **(A) STAT3:** IL-6 stimulation did not induce activation of STAT3 in undifferentiated MSCs. Activated STAT3 (STAT3 (P)) was only observed in the positive control lysates, while total STAT3 levels remained constant with IL-6 treatment. Actin is shown as a loading control. **(B) ERK1/2:** Serum-starved MSCs have baseline activation of ERK1/2 (ERK1/2 (P)), which increased after 5 min of IL-6 stimulation, before returning to baseline levels at 60 min. Actin is shown as a loading control. **(C) U0126 inhibition:** IL-6-induced ERK1/2 activation (ERK1/2 (P) in undifferentiated MSCs was inhibited by U0126. Actin is shown as a loading control. **(D-G) Effect of ERK1/2 inhibition:** (D) IL-6 alone significantly increased proliferation over controls, while IL-6 stimulation in the presence of U0126 failed to induce an increase in proliferation (N=3). (E, F) *LPL* and *FABP4* mRNA levels were decreased by day 14 in cells differentiated after exposure to IL-6; *LPL* and *FABP4* expression was increased in cells differentiated after exposure to IL-6+U0126 (N=3). (E) *COL2A1* gene expression in MSCs pre-treated with vehicle (Control), IL-6, or IL-6+U0126. All real-time RT-PCR data shown are normalized against *GAPDH* (ANOVA: * $p < 0.05$, ** $p < 0.01$, *** $p < 0.001$).